Inorganic Chemistry

Article

pubs.acs.org/IC

Studies of Cobalt-Mediated Electrocatalytic CO_2 Reduction Using a Redox-Active Ligand

David C. Lacy, Charles C. L. McCrory, and Jonas C. Peters*

Joint Center for Artificial Photosynthesis, Division of Chemistry and Chemical Engineering, California Institute of Technology, Pasadena, California 91125, United States

Supporting Information

ABSTRACT: The cobalt complex $[Co^{III}\mathbf{N_4H}(Br)_2]^+$ ($\mathbf{N_4H}$ = 2,12-dimethyl-3,7,11,17-tetraazabicyclo-[11.3.1]-heptadeca-1(7),2,11,13,15-pentaene) was used for electrocatalytic CO_2 reduction in wet MeCN with a glassy carbon working electrode. When water was employed as the proton source (10 M in MeCN), CO was produced (f_{CO}= 45% ± 6.4) near the $Co^{I/0}$ redox couple for $[Co^{III}\mathbf{N_4H}(Br)_2]^+$ ($E_{1/2}$ = −1.88 V $FeCp_2^{+/0}$) with simultaneous H_2 evolution (f_{H2}= 30% ± 7.8). Moreover, we successfully demonstrated that the catalytically active species is homogeneous through the use of control experiments and XPS studies of the working glassy-carbon electrodes. As determined by cyclic voltammetry, CO_2 catalysis occurred near the formal $Co^{I/0}$redox couple, and attempts were made to isolate the triply reduced compound ("$[Co^0\mathbf{N_4H}]$"). Instead, the doubly reduced ("Co^I") compounds $[Co\mathbf{N_4}]$ and $[Co\mathbf{N_4H}(MeCN)]^+$ were isolated and characterized by X-ray crystallography. Their molecular structures prompted DFT studies to illuminate details regarding their electronic structure. The results indicate that reducing equivalents are stored on the ligand, implicating redox noninnocence in the ligands for H_2 evolution and CO_2 reduction electrocatalysis.

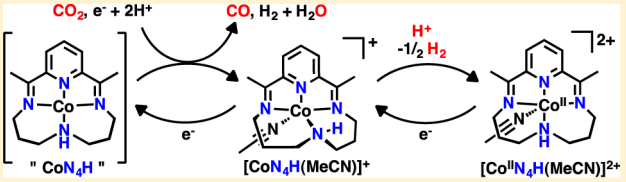

INTRODUCTION

Transition metal complexes supported by nitrogen-donor ligands constitute an important class of molecular electrocatalysts for CO_2reduction.[1] Whereas the earliest report featured phthalocyanine as a supporting ligand, a host of nitrogen-rich donor ligands have since been employed that include porphyrins,[3] polypyridines,[4] cyclam, and related unsaturated N_4-macrocycles.[5] Convincing evidence has been provided in support of a hypothesis whereby reducing equivalents are stored on supporting polypyridine ligands during electrocatalytic CO_2 reduction.[6] Redox noninnocence at the ligand may have a significant impact on both substrate and product selectivity.[7] For example, bipyridyl-supported manganese and rhenium tricarbonyl catalysts reduce CO_2 rather than protons in the presence of water and/or weak acids.[8] These findings encouraged our interest in exploring the importance of redox noninnocent ligand properties in electrocatalytic CO_2 reductions.

In the present study we continue the theme of elucidating a role for ligand redox noninnocence in the context of electrocatalytic CO_2 reduction by cobalt. We employ the ligand $\mathbf{N_4H}$ ($\mathbf{N_4H}$ = 2,12-dimethyl-3,7,11,17-tetraazabicyclo-[11.3.1]-heptadeca-1(7),2,11,13,15-pentaene), chosen because it contains a potentially redox-active pyridyldiimine (PDI) moiety.[9,10] Additionally, there is literature precedent for electrocatalytic CO_2 reduction with the PDI platform with cobalt.[11] In particular, three prior studies employed the $\mathbf{N_4H}$ ligand for electrocatalytic CO_2 reduction and showed production of large amounts of H_2 relative to CO and low overall current efficiencies.[5a,12] The latter observation is consistent with appreciable current being consumed to reductively degrade the molecular precursor. The catalytic role of resulting heterogeneous material must therefore be considered but was difficult to assess owing to the choice of mercury as the working electrode. Mercury electrodes are known to strongly adsorb N_4-macrocyclic cobalt complexes,[13] and there has been significant discussion about the activity of dissolved molecular complexes versus mercury adsorbed species in catalysis.[14,15] Reports that some nominally discrete homogeneous molecular cobalt-based electrocatalysts form catalytically active heterogeneous deposits, even on glassy carbon electrode surfaces, encourage added caution to be taken when defining likely contributors to observed overall electrocatalysis.[16]

The present combined synthetic/electrocatalytic study employs a glassy-carbon working electrode to investigate the cobalt-$\mathbf{N_4H}$ system for CO_2 reduction. The lead observation made pertains to preferential CO_2 reduction (to produce CO) relative to H_2 evolution when wet organic solvent is used. To begin to develop a better understanding of this system, synthetic studies are described wherein reduced and protonated cobalt species that we presume are relevant to overall electrocatalysis are characterized. The structural data obtained for these species are correlated to DFT calculations and suggest that redox noninnocent ligand behavior is likely operative. Of course, the molecular studies described are directly relevant to the overall CO_2 reduction electrocatalysis only if homogeneous

Received: December 30, 2013
Published: April 28, 2014

   dx.doi.org/10.1021/ic403122j | Inorg. Chem. 2014, 53, 4980−4988

catalysis is operative. Several control experiments support a dominant role for homogeneous species in the observed CO_2 electrocatalysis, despite the fact that some heterogeneous cobalt material forms on the electrode surface during electrocatalysis.

RESULTS

Electrocatalytic CO_2 Reduction with $[Co^{III}N_4H(Br)_2]^+$ in Wet MeCN. Cyclic voltammograms (CVs) of 0.3 mM solutions of $[Co^{III}N_4H(Br)_2]^+$ with nBu$_4$NPF$_6$ in MeCN were measured (Figure 1), and three reversible redox couples were

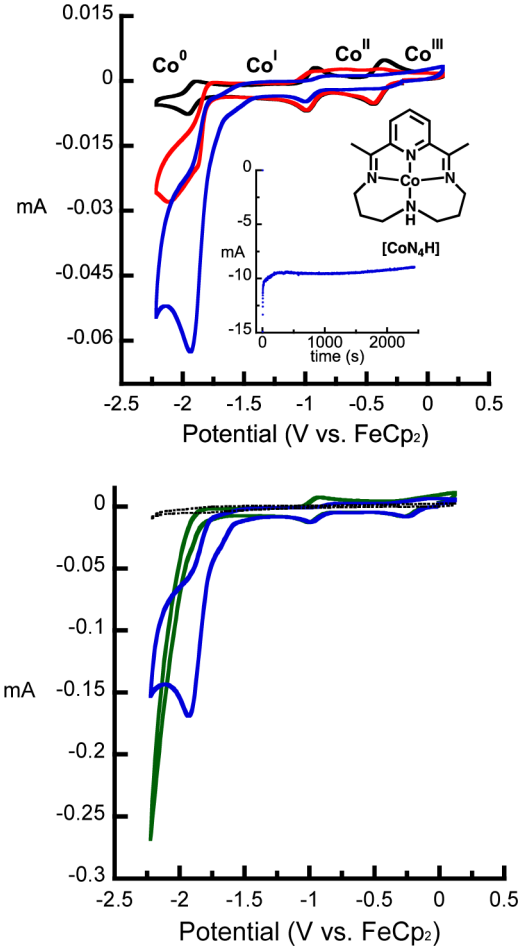

Figure 1. (Top) Cyclic voltammograms of 0.3 mM $[Co^{III}N_4H(Br)_2]^+$ in MeCN (black), addition of CO_2 (red), and addition of water to make a 10 M solution in MeCN (blue). Inset shows a plot of current vs time for a 40-min controlled potential electrolysis experiment (potential held at −2.13 vs $FeCp_2^{+/0}$). (Bottom) CV of 0.7 mM $[Co^{III}N_4H(Br)_2]^+$ in MeCN with 10 M H_2O with CO_2 (blue) and without CO_2 (green); the dashed black line is the background current in MeCN with 10 M H_2O and CO_2 with no added cobalt complex. Conditions: scan rate = 0.100 V/s; supporting electrolyte is 0.1 M nBu$_4$NPF$_6$; working electrode = glassy carbon; reference electrode = isolated Ag/AgNO$_3$ (1 mM) with 0.1 M nBu$_4$NPF$_6$; counter electrode = glassy carbon.

observed at −0.40 V, −0.92 V, and −1.88 V (all potentials are referenced to the $FeCp_2^{+/0}$ couple). These redox events are assigned as the formal $Co^{III/II}$, $Co^{II/I}$, and $Co^{I/0}$ couples, respectively. When MeCN solutions of $[Co^{III}N_4H(Br)_2]^+$ were saturated with CO_2, an increase in the magnitude of the reductive current appeared near the $Co^{I/0}$ couple, suggesting the possibility of catalytic activity. Adding water increased the magnitude of the catalytic wave near the $Co^{I/0}$ couple in the CV (Figure 1). A different current response was observed when no CO_2 was present (Figure 1, bottom). These findings are generally consistent with an early study by Tinnemans et al. in 1984, where it was first demonstrated that CVs of $[Co^{III}N_4H(Br)_2]^+$ were affected by CO_2 and that H_2O could enhance the catalytic wave.[12a]

Tinnemans et al. and Che et al. performed controlled potential electrolysis (CPE) experiments under various conditions, and CO was produced in 20−30% Faradaic efficiency at −1.8 V in MeCN with water concentrates as high as 3 M (Table S2 in the Supporting Information [SI]). We obtained similar results and observed turbid solutions after an extended 40 min CPE in MeCN with water concentrations as low as 0.035 ± 4 M (measured by Karl Fischer) and likewise obtained low total current efficiencies for CO (f_{CO} = 24%) and little to no H_2 (f_{H2} = <1%). However, increasing the water concentration to 10 M gave substantially higher Faradaic efficiencies for CO (f_{CO} = 45% ± 6.4), with H_2 production (f_{H2} = 30% ± 7.8) (Table 1).[17] The solutions with 10 M H_2O did not become turbid, and a UV−vis spectrum of the working solution after a CPE displayed features that were similar to those observed for $[Co^{II}N_4H(Br)]^+$ and $[Co^{II}N_4H(MeCN)]^{2+}$ (*vida infra*) (Figure S1 in the SI); though quantification was not possible because the exact speciation could not be established, the spectrum indicates that a $[Co^{II}N_4H]^{2+}$ complex is the majority species present. Over the course of these 40-min CPE experiments 22 ± 3.2 C were passed, and a plot of current vs time was relatively constant (Figure 1, inset). These data correspond to a TON_{CO} of 4.1 ± 0.9 and TON_{H2} of 2.8 ± 1.0. In contrast to the original report,[12a] no formate or oxalate was detected under any set of conditions. Substitution of CO_2 with $NaHCO_3$ (30 mM, saturated) in bulk electrolysis experiments did not yield any reduced CO_2 products.

Table 1. Results of Controlled Potential Electrolysis (CPE) Experiments Held at −2.0 V vs a Ag/AgNO$_3$ Reference Electrode[a] for 40 Min

comments	q/ C	f_{CO}/ %	f_{H2}/ %
$[CoN_4H(Br)_2]^+$ in MeCN (10 M H_2O) w/ CO_2	22 ± 3.2	45 ± 6.4	30 ± 7.8
$[CoN_4H(Br)_2]^+$ in MeCN (10 M H_2O) w/o CO_2	40 ± 4.5	0	63 ± 3.5
$CoCl_2$ in MeCN (10 M H_2O) w/ CO_2	6.9 ± 0.4	<1%	83 ± 4.0
background in MeCN (10 M H_2O) w/CO_2 w/**bare electrode**	2.1 ± 1.3	<1%	61 ± 13*
background in MeCN (10 M H_2O) w/ CO_2 w/ **used electrode**	2.9 ± 1.3	<1%	66 ± 17*

[a]The reference electrode was externally referenced to a solution containing ferrocene in MeCN with 0.1 M nBu$_4$NClO$_4$. The $FeCp_2^{0/+}$ couple occurred at 0.13 V. See Experimental Section for conditions. *The hydrogen detected was near the detection limit of the GC (~1000 ppm) and accounts for the large error.

It has been previously reported that, in the case of hydrogen evolution by a *tris*(glyoximate) cobalt clathro chelate precatalyst complex, the catalytic species is a cobaltous material electrodeposited onto the electrode surface at negative potentials rather than the molecular complex.[16a] To test whether the catalytic species in the present study might be an electrodeposited film, the electrode surface was probed with XPS, and several informative control experiments were conducted. After a

dx.doi.org/10.1021/ic403122j | Inorg. Chem. 2014, 53, 4980−4988

CPE experiment, the electrode was removed and washed with fresh acetonitrile and water, and the surface was then probed by XPS. A very low coverage of <0.3 atom % cobalt was found on the surface (Figure S2 and S3, Table S3 in the SI), corresponding to a Co/C ratio of <0.004. For comparison, a monolayer coverage of e-beam deposited Co on SiO_2 has a Co/Si ratio of ~0.1,[19] and a monolayer coverage of electrodeposited Co oxide on Au has a Co/Au ratio of ~1.4.[20] This suggests that there is significantly less than a monolayer coverage of Co deposited onto the glassy carbon electrodes post-CPE, although rigorous quantification of Co coverage would require additional experiments beyond the scope and intent of this manuscript. To test whether the deposited material was catalytically active, electrodes that were used for CPE experiments with $[Co^{III}N_4H(Br)_2]^+$ were rinsed with fresh acetonitrile and water, and an additional 40 min electrolysis was run under identical conditions, except that the precatalyst $[Co^{III}N_4H(Br)_2]^+$ was not added to the solution. For these background experiments with the "used electrodes", 2.9 ± 1.3 C of charge were passed with f_{CO} = <1%. The results are similar to those obtained from the background CPE experiments in which a clean unused electrode was used with no dissolved precatalyst (2.1 ± 1.3 C, f_{CO} = <1%). For these control experiments, the amount of charge passed is appreciably less than those containing dissolved precatalyst complex (22 ± 3.2 C), and more importantly, selectivity for CO_2 over H^+ is dramatically enhanced in the presence of $[Co^{III}N_4H(Br)_2]^+$. We also performed control CPE experiments with dissolved $CoCl_2$ which formed turbid solutions and produced H_2 in f_{H2} = 83% ± 4.0 and f_{CO} = <1% (6.9 ± 0.4 C). Note that it is known that $CoCl_2$ deposits cobalt material on glassy carbon.[16c] These observations provide evidence that any cobalt material deposited on the electrode is not responsible for the observed CO_2 reduction catalysis and that a molecular cobalt–$\mathbf{N_4H}$ complex is involved in the electrocatalytic process.

Synthesis and Molecular Structure of [CoN$_4$]. Considering that electrocatalytic CO_2 reduction occurred at a potential very close to the $Co^{I/0}$ couple, we endeavored to isolate the reduced species and study its stoichiometric reactions with CO_2. This was accomplished by using $[Co^{II}N_4H(Br)]Br$ as a synthon.[21] Reduction of $[Co^{II}N_4H(Br)]Br$ with 2 equiv KC_8 in THF afforded a dark-purple, benzene soluble product that analyzed as [CoN$_4$] (Scheme 1).[22] The ^1H NMR spectrum of [CoN$_4$] in C_6D_6 is that of a diamagnetic species and contains four aliphatic and two aromatic C–H resonances but is missing the resonance expected for the NH group of the $\mathbf{N_4H}$ ligand (Figure S4 in the SI).[23] Further indication of the absence of an N–H bond comes from the lack of a ν(NH) in the FTIR-ATR spectrum of [CoN$_4$] (Figure S5 in the SI). Crystals suitable for X-ray diffraction were obtained by slow diffusion of pentane into a concentrated benzene solution of [CoN$_4$].

The molecular structure of [CoN$_4$] revealed that the cobalt ion is four-coordinate and distorted square planar (Figure 2).

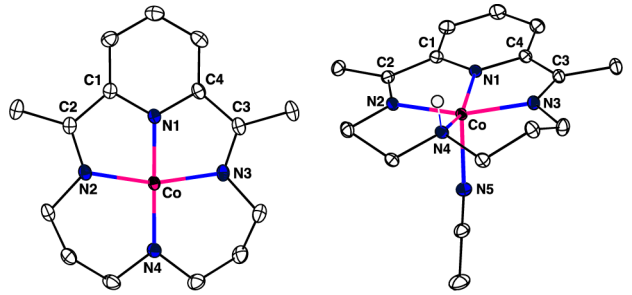

Figure 2. X-ray crystal structure of [CoN$_4$] (left) and $[CoN_4H(MeCN)]^+$ (right). Except for the NH group, hydrogen atoms are removed for clarity. Thermal ellipsoids displayed at 50% probability. The $[BPh_4]^-$ counteranion in $[CoN_4H(MeCN)][BPh_4]$ has been removed for clarity.

The amido nitrogen N4 is planar (Σ∠ = 360.0°), and no hydrogen was found in the difference map. The cobalt-pyridine Co1–N1 bond distance is 1.800(2) Å, a contraction compared to 1.848(1) Å in $[Co^{II}N_4H(MeCN)]^{2+}$ (*vide infra*; Table 2).

Table 2. Comparison of metrical parameters from XRD data for [CoN$_4$], $[CoN_4H(MeCN)]^+$, and $[Co^{II}N_4H(MeCN)]^{2+}$

	[CoN$_4$]	$[CoN_4H(MeCN)]^+$	$[Co^{II}N_4H(MeCN)]^{2+}$
	Bond Distances (Å)		
Co1–N1	1.800(2)	1.807(1)	1.848(1)
Co1–N2	1.881(2)	1.920(1)	1.957(1)
Co1–N3	1.888(2)	1.921(1)	1.971(1)
Co1–N4	1.810(2)	2.023(1)	1.966(1)
N2–C2	1.330(2)	1.319(2)	1.303(2)
N3–C3	1.330(2)	1.325(2)	1.294(2)
Co1–N5	–	1.998(1)	2.105(1)
C1–C2	1.442(2)	1.444(2)	1.476(3)
C3–C4	1.436(2)	1.435(2)	1.474(3)
	Bond Angles (deg)		
N1–Co–N4	178.81(5)	155.48(2)	172.671(4)
N2–Co–N3	162.91(5)	160.92(2)	162.101(3)

Similarly short Co–N_{py} bond distances of 1.787(2) Å and 1.797(3) Å were observed for the related [PDI]CoCl complexes.[24,25] For [CoN$_4$], the Co1–N1 contraction is accompanied by a shortening of the Co1–$N4_{(amido)}$ distance to 1.810(2) Å, down from 1.966(1) Å in $[Co^{II}N_4H(MeCN)]^{2+}$. Compared to other cobalt–amido bond distances, the Co1–N4 distance in [CoN$_4$] is unusually short. For comparison, Fryzuk et al. has characterized several high-spin $[Co^{I}PNP]$ complexes with Co–N_{amido} bond distances ranging from 1.898(3) to 1.904(3) Å.[26] Caulton and co-workers have reported a three coordinate S = 1 $[Co^{I}PNP]$ complex which has a Co–N_{amido} bond distance of 1.973(2) Å that shortens by ~0.03 Å when CO is bound.[27a] Additionally, Mindiola and co-workers synthesized a different $[Co^{I}PNP]_2(\mu\text{-}N_2)$ complex with a Co–N_{amido} distance of 1.928(2) Å.[27b] Except for $[Co^{I}PNP(CO)]$ and $[Co^{I}PNP]_2(\mu\text{-}N_2)$, the difference in spin state (paramagnetic $[Co^{I}PNP]$ vs diamagnetic [CoN$_4$]) makes it difficult to meaningfully compare these bond distances to those in [CoN$_4$]. Finally, the imine C–N bond distances (1.330(2)

Scheme 1. Synthesis of [CoN$_4$], $[CoN_4H(MeCN)]^+$, and $[Co^{II}N_4H(MeCN)]^{2+}$[a]

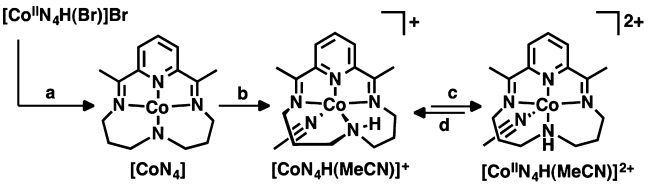

[a]Conditions: (a) $2KC_8$, THF, RT; (b) $NaBPh_4$, $MeCN/H_2O$ (3:1), RT; (c) [H-DMF][OTf], MeCN, RT; (d) electrochemical reduction, $E_{1/2}$ = −0.92 V vs $FeCp_2^{+/0}$.

dx.doi.org/10.1021/ic403122j | Inorg. Chem. 2014, 53, 4980–4988

Å) in [Co$\mathbf{N_4}$] are longer than expected for a redox-innocent PDI moiety, which complicates the oxidation state assignment of the cobalt ion and is discussed further below.

Synthesis and Molecular Structure of [Co$\mathbf{N_4}$H(MeCN)]$^+$. We investigated the possibility of isolating the protonated form of [Co$\mathbf{N_4}$]. This was accomplished by dissolving purple [Co$\mathbf{N_4}$] in a 3:1 MeCN/H_2O mixture, affording a dark-forest green solution (Scheme 1). The new species [Co$\mathbf{N_4H}$(MeCN)][BPh_4] was isolated in 65% yield by precipitation with $NaBPh_4$. The ^{1}H NMR spectrum of [Co$\mathbf{N_4H}$(MeCN)]$^+$ contains sharp resonances in the diamagnetic region and includes a resonance at 2.43 ppm (1H, t, J_{N-H} = 11.5 Hz) that integrates to one proton. This resonance is greatly diminished in the ^{1}H NMR spectrum of the isotopomer [Co$\mathbf{N_4D}$(MeCN)]$^+$ (Figure S6 in the SI). The FTIR-ATR spectrum of [Co$\mathbf{N_4H}$(MeCN)]$^+$ contains an isotopically sensitive ν(NH) band at 3250 cm^{-1} that shifts to 2415 cm^{-1} when [Co$\mathbf{N_4D}$(MeCN)]$^+$ is used (ν(NH)/ ν(ND) = 1.345; calcd = 1.370) (Figure S5 in the SI).

The X-ray crystal structure of the cation [Co$\mathbf{N_4H}$(MeCN)]$^+$ reveals a five-coordinate distorted square pyramidal (τ = 0.09) cobalt ion bound to $\mathbf{N_4H}$ (Figure 2). In contrast to [Co$\mathbf{N_4}$], the amine nitrogen N4 is protonated and pyramidalized ($\Sigma\angle$ = 338.8°). The Co1−N1 bond distance in [Co$\mathbf{N_4H}$(MeCN)]$^+$ is 1.807(1) Å, similar to that found in [Co$\mathbf{N_4}$]. However, in [Co$\mathbf{N_4H}$(MeCN)]$^+$ the Co1−N4 bond is elongated to 2.023(1) Å reflecting the protonation of the amido ligand. An acetonitrile molecule occupies the fifth coordination site of the cobalt ion. As with [Co$\mathbf{N_4}$], the C2−N2 and C3−N3 imine bond lengths in [Co$\mathbf{N_4H}$(MeCN)]$^+$ are elongated to 1.319(2) Å and 1.325(2) Å, respectively, compared to those in [Co$^{II}\mathbf{N_4H}$(MeCN)]$^{2+}$.

Synthesis and Molecular Structure of [Co$^{II}\mathbf{N_4H}$(MeCN)]$^{2+}$. We explored the stoichiometric reactivity of [Co$\mathbf{N_4H}$(MeCN)]$^+$ with acid. Treating [Co$\mathbf{N_4H}$(MeCN)]$^+$ with one equivalent of [H-DMF][OTf] (pK_a = 6.1)[28] in MeCN resulted in an immediate color change from dark-forest green to orange-red. The headspace of the reaction analyzed by GC confirmed production of 1/2 equiv H_2 (47% ± 4). A similar experiment was performed in a sealed J-young tube with [H-DMF][OTf] and [Co$\mathbf{N_4D}$(MeCN)]$^+$, and it was found that the ^{1}H NMR spectrum contained an H_2 resonance but showed no evidence of coupling from incorporation of deuterium. *This result suggests that the proton on the $\mathbf{N_4H}$ ligand is not incorporated into the H_2 product.*

The orange-red solution resulting from treatment of [Co$\mathbf{N_4H}$(MeCN)]$^+$ with [H-DMF][OTf] contained a paramagnetic S = 1/2 cobalt complex (μ_{eff} = 1.6 μ_B, RT in CD_3CN). This conclusion is supported by the 77 K EPR spectrum (Figure S7 in the SI) of a frozen solution of the purified material, which was isolated in 87% yield and analyzed as [Co$^{II}\mathbf{N_4H}$(MeCN)][OTf][BPh_4]. The UV−vis and EPR spectra of the product are nearly identical to those very recently reported by Deronzier and co-workers (Figure S8 in the SI) in the context of photochemical H_2 production.[30] The molecular structure of [Co$^{II}\mathbf{N_4H}$(MeCN)]$^{2+}$ was determined by X-ray diffraction and revealed a five-coordinate (τ = 0.18) cobalt complex with two outer sphere anions (Figure 3). The amine on $\mathbf{N_4H}$ is H-bonded to the triflate anion as indicated from the N4···O1 distance of 2.844(2) Å. Compared to [Co$\mathbf{N_4}$] and [Co$\mathbf{N_4H}$(MeCN)]$^+$, the complex [Co$^{II}\mathbf{N_4H}$(MeCN)]$^{2+}$ has noticeably shorter imine C−N bond lengths (1.303(2) Å and 1.294(3) Å) (Table 2). These shorter bond lengths are consistent with the spectroscopic assignment of the product being a Co^{II} ion bound to the neutral ligand $\mathbf{N_4H}$.

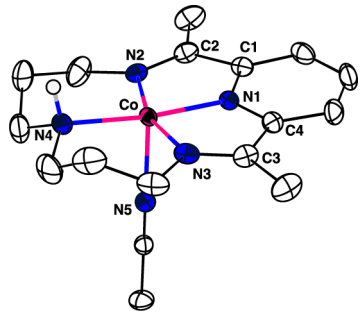

Figure 3. X-ray crystal structure of [Co$^{II}\mathbf{N_4H}$(MeCN)]$^{2+}$. Except for the NH group, hydrogen atoms are removed for clarity. Thermal ellipsoids displayed at 50% probability. The [BPh_4]$^-$ and [OTf]$^-$ counteranions in [Co$^{II}\mathbf{N_4H}$(MeCN)][OTf][BPh_4] have been removed for clarity.

Electrochemical Properties of [Co$\mathbf{N_4H}$(MeCN)]$^+$ and [Co$^{II}\mathbf{N_4H}$(MeCN)]$^{2+}$ and Electrocatalytic H_2 Evolution. We also probed the electrochemical properties of [Co$\mathbf{N_4H}$(MeCN)]$^+$ and [Co$^{II}\mathbf{N_4H}$(MeCN)]$^{2+}$. The CV of [Co$\mathbf{N_4H}$(MeCN)]$^+$ (Figure 4) exhibits two reversible couples,

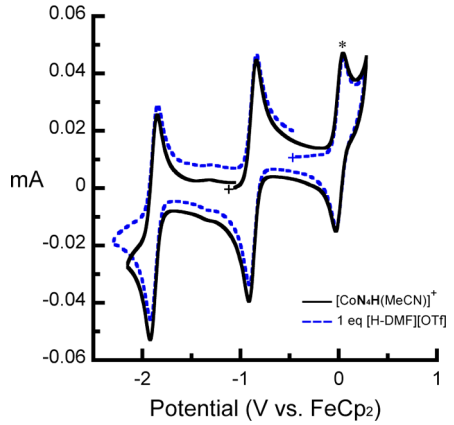

Figure 4. CV of 1 mM [Co$\mathbf{N_4H}$(MeCN)]$^+$ in MeCN before (black) and after (dashed blue) addition of 1 equiv [H-DMF][OTf]. Conditions: 0.1 M nBu$_4$NPF$_6$; reference electrode = silver wire (* = internal $FeCp_2$).

one oxidation at −0.88 V vs $FeCp_2^{+/0}$ (formally the Co$^{I/II}$ couple) and one reduction at −1.88 V vs $FeCp_2^{+/0}$ (formally the Co$^{I/0}$ couple).[31] Addition of 1 equiv [H-DMF][OTf] caused the solution to turn orange red, but there was no change in the CV except that the resting state potential shifted positive of the redox couple at −0.88 V, indicative of an oxidation state change. Notably, addition of excess [H-DMF][OTf] or tosic acid (TsOH·H_2O) resulted in the formation of a catalytic wave near the Co$^{II/I}$ couple consistent with electrocatalytic H_2 evolution (Figure S9 in the SI). CPE experiments were conducted at two potentials for TsOH·H_2O (pK_a = 8)[32] and 2,6-dichloroanalinium tetrafluoroborate ([2,6-DCA][BF_4], pK_a = 5.1),[33] the results of which are presented in Table S4 in the SI. These experiments confirm H_2 as the major product with >85% Faradaic efficiency.

dx.doi.org/10.1021/ic403122j | Inorg. Chem. 2014, 53, 4980−4988

DISCUSSION

The CVs of $[Co^{III}N_4H(Br)_2]^+$ in the presence of CO_2 indicated that CO_2 reacts at the formal "$Co^{I/0}$" couple. On the basis of the reversibility of this couple and on the successful isolation of the $[NiN_4H]$ complex,[10] we anticipated that treatment of cobalt−N_4H complexes with the appropriate stoichiometric reductant would produce an analogous $[CoN_4H]$ complex. However, in all attempts the only tractable cobalt-containing product was $[CoN_4]$. To summarize, treatment of either $[Co^{II}N_4H(Br)]^+$ or $[Co^{II}N_4H(MeCN)]^{2+}$ with 2 equiv KC_8 or NaHg only formed $[CoN_4]$. The same occurred when 1 equiv KC_8 was reacted with $[CoN_4H(MeCN)]^+$. The mechanism by which $[CoN_4]$ is formed is not known; however, a cobalt-hydrido species may result from isomerization of $[CoN_4H]$ and subsequently lose H• bimolecularly in the form of H_2 (Scheme 2).[22] This contrasts the stability of $[NiN_4H]$, which does not appear to lose H_2 to form the corresponding $[NiN_4]$ complex.

Scheme 2. Plausible Outline for CO_2 Reduction Involving the Putative "$[CoN_4H]$" Complex That Is Formed at the Formal $Co^{I/0}$ Redox Couple; the "$[CoN_4H]$" Complex Is Unstable to Loss of H_2 but Can Be Intercepted by CO_2

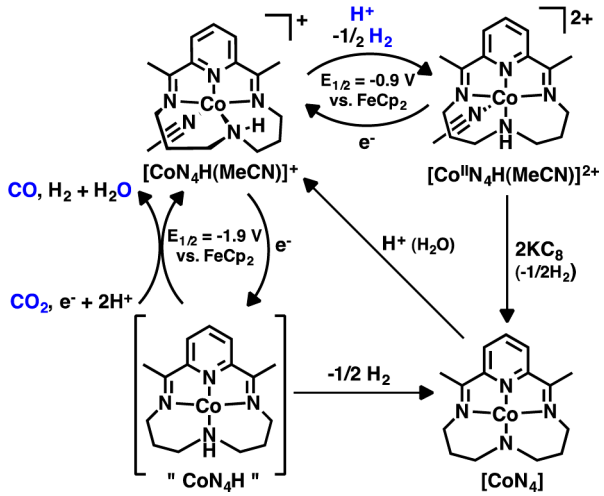

This loss of H_2 at the $Co^{I/0}$ redox event may be a consequence of ligand noninnocence and its interaction with the cobalt ion. To probe this possibility, we explored the electronic structures of the reduced complexes we prepared. On the basis of the charge of $[CoN_4]$ and $[CoN_4H(MeCN)]^+$, the cobalt ions are in the +1 oxidation state. However, the imine C−N bond distances suggest a more complicated description of the electronic structures. Several research groups have investigated [PDI]CoX (X = halide, alkyl, H) complexes.[9,10,24,25] From these studies, the sum of the results suggest that the electronic environments of [PDI]CoX species (formally Co^I) are usually best described as having an open-shell singlet configuration in which a low-spin Co^{II} ion is antiferromagnetically coupled to a ligand-based anion radical.[24,25] The $[NiN_4H]$ complex, that Wieghardt and co-workers have characterized, formally contains a "Ni^0" ion but has elongated imine C−N bond lengths (1.353(7) Å and 1.351(8) Å).[10] Along with DFT studies, the complex $[NiN_4H]$ was interpreted as containing a Ni^{II} ion bound to the dianionic ligand N_4H^{2-}. The imine C−N bond lengths of $[CoN_4]$ and $[CoN_4H(MeCN)]^+$ are in between those of $N_4H^{2-}$and N_4H, and close to those in the [PDI]CoX complexes, suggesting a description for $[CoN_4]$ having a Co^{II} ion bound to $N_4^{\bullet-}$ (and $N_4H^{\bullet-}$ for $[CoN_4H(MeCN)]^+$).

To supplement the crystallography, we also performed DFT calculations on $[CoN_4]$ and $[CoN_4H(MeCN)]^+$ and found that in both cases the open-shell singlet configuration was 4.4 and 4.6 kcal/mol, respectively, lower in enthalpy than the closed-shell configuration. A surface plot of the atomic spin density (Figure 5) supports the hypothesis that an anion radical ($N_4^{\bullet-}$, $N_4H^{\bullet-}$) is antiferromagnetically coupled to a low-spin Co^{II} ion. For $[CoN_4]$ and $[CoN_4H(MeCN)]^+$, the atomic spin-density on the cobalt ion is 0.75 and 0.81, respectively, with the remaining spin density distributed throughout the ligand.

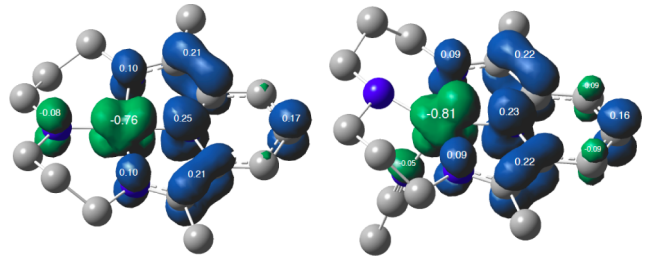

Figure 5. Mulliken atomic spin-density surface of $[CoN_4]$ (left) and $[CoN_4H(MeCN)]^+$ (right) (isovalue = 0.003). Hydrogen atoms removed for clarity.

The redox noninnocence of N_4H may have implications on selectivity between H_2 evolution and CO_2 reduction electrocatalysis. This is important because the difficulty of decoupling CO_2 reduction from H_2 evolution remains an outstanding challenge in electrocatalysis. For example, some of the better H_2-evolving molecular electrocatalysts are cobalt N_4-macrocyles with imino-glyoximate ligands.[34] However, to our knowledge there are no reports of successful electrocatalytic CO_2 reduction using cobalt complexes with these ligands.[35] Recent investigations into the electronic structure of reduced cobalt and nickel complexes with imino-glyoximate ligands have suggested redox noninnocence, albeit with deleterious side reactions resulting in ligand modification.[36] Including this report, previous investigations from Peters,[34i] Deronzier[30] and Lau[37] have demonstrated that $[Co^{III}N_4H(X)_2]^+$ (X = halogen) is a competent precatalyst for H_2 evolution. It was therefore surprising that $[Co^{III}N_4H(Br)_2]^+$ is a competent precatalyst for CO_2 reduction under the appropriate conditions. The stability of the reduced $N_4H^{\bullet-}$ ligand radical anion, and perhaps the ability to accommodate a second redox equivalent as demonstrated by $[NiN_4H]$, likely contributes to preferential CO_2 reduction in wet MeCN. Although the putative $[CoN_4H]$ complex is unstable to loss of H_2, the electrogenerated $[CoN_4H]$ intermediate is at least sufficiently stable under electrocatalytic conditions to be intercepted by CO_2 (Scheme 2). The mechanism by which CO and H_2 are formed, either by two competing or one synchronous path, is still undetermined and currently under investigation.

CONCLUSIONS

In this report, we have explored the CO_2 reduction activity of a cobalt complex with a redox active pyridyldiimine moiety. In particular, we have shown that the formally "Co^I" complex $[CoN_4H(MeCN)]^+$ is a precatalyst for the reduction of CO_2 to CO in CO_2-saturated solutions of MeCN with 10 M H_2O (f_{CO} = 45% ± 6.4), and does so preferentially to H^+ reduction even

dx.doi.org/10.1021/ic403122j | Inorg. Chem. 2014, 53, 4980−4988

though the complex is known to be competent for electrocatalytic H_2-evolution. XPS measurements of glassy carbon electrodes post-CPE and other control experiments support the assertion that the dissolved molecular complex, rather than an electrodeposited film, is responsible for the observed electrocatalysis. In addition, we have isolated the formally "Co^{I}" complex $[Co\mathbf{N_4H}(MeCN)]^+$ by protonation of the "Co^{I}"–amido complex $[Co\mathbf{N_4}]$, both of which were characterized by X-ray crystallography. Along with the molecular structures, broken symmetry DFT calculations suggest they are nominally described as low-spin Co^{II} ions antiferromagnetically coupled to a ligand radical-anion ($\mathbf{N_4H^{\bullet -}}$ and $\mathbf{N_4^{\bullet -}}$), a result consistent with the [PDI]CoX literature.[9] The stability of the $\mathbf{N_4H^{\bullet -}}$ ligand radical anion and ability to accommodate a second redox equivalent may contribute to the preferential reduction of CO_2 over H^+ in the presence of large concentrations of water.

EXPERIMENTAL SECTION

General and Physical Methods. All reagents were purchased from commercial sources and used as received unless otherwise noted. Solvents were sparged with nitrogen and dried over columns containing molecular sieves or alumina. The deuterated solvents were degassed and dried over activated 3 Å sieves prior to use. NMR spectra were recorded on Varian 300, 400, and 500 MHz spectrometers. ^1H and ^{13}C chemical shifts are reported in ppm relative to residual solvent as internal standards and are singlets unless otherwise stated. Identification of ^{13}C shifts were made on the basis of standard 2D methods (HSQC and HMBC). Elemental analyses were performed on a Perkin Elmer 2400 CHNS analyzer. Electronic absorbance spectra were recorded with a Cary 50 spectrometer. Fourier transform infrared ATR spectra were collected on a Thermo Scientific Nicolet iS5 spectrometer with diamond ATR crystal (utilized iD5 ATR insert). GC measurements were collected using an Agilent Technologies 7890A GC system with front and back TCD channels. X-band EPR spectra were recorded on a Bruker EMX spectrometer. Electrochemical experiments were conducted using a Biologic VSP-300 five-channel potentiostat using the EC Lab Express version 5.53 software package.

Electrochemical Methods. *Cyclic Voltammetry.* Unless otherwise stated, the working electrode was a 0.071 cm^2 diameter glassy carbon disk electrode (CH instruments), and the counter electrode was carbon rod (99.999% Strem). The reference electrode was a $Ag/AgNO_3$ (1.0 mM)/MeCN nonaqueous reference electrode (also contained 0.1 M nBu$_4$NPF$_6$) separated from the solution by a Vycor frit (Bioanalytical Systems, Inc.) and externally referenced to ferrocene. Alternately, the reference electrode was a silver wire with an internal ferrocene standard (internally referenced CVs contain an asterisk indicating the $FeCp_2^{+/0}$ couple).

Controlled-Potential Electrolysis. Controlled-potential electrolysis experiments were conducted at ambient pressure in a sealed two-chamber cell where the first chamber held the working and reference electrodes in 40 mL of 0.1 M nBu$_4$NClO$_4$ in MeCN with 0.3 mM catalyst, and the second chamber held the auxiliary electrode in 19 mL of 0.1 M nBu$_4$NClO$_4$ in MeCN with 20 mM $FeCp_2$. The two chambers were separated by a fine porosity glass frit. A 6 cm × 1 cm × 0.3 cm glassy carbon plate (Tokai Carbon U.S.A.) was used as the working electrode, about a quarter of which was submerged in the solution. The auxiliary electrode was a nichrome wire (EISCO scientific). The reference electrode was a $Ag/AgNO_3$ (1 mM)/MeCN nonaqueous reference electrode separated from the solution by a Vycor frit (Bioanalytical Systems, Inc.) and contained 0.1 M nBu$_4$NClO$_4$. The cell was prepared with degassed solvent on a Schlenk line with N_2 or CO_2 for 30 min and then sealed before the beginning of each controlled-potential electrolysis experiment. Each controlled-potential electrolysis experiment was conducted for 40 min at the specified potential (−2.0 V vs the $Ag/AgNO_3$ reference electrode) under vigorous stirring (the stir plate was set to 900 rpm). The amount of CO and H_2 evolved was quantified from an analysis of the headspace with an Agilent 7890A gas chromatograph using a thermal conductivity detector. Faradaic efficiencies were determined by dividing the measured CO and H_2 produced by the amount of CO and H_2 expected on the basis of the charge passed during the controlled-potential electrolysis measurement.

X-ray Photoelectron Spectroscopy. The surface composition of the carbon electrode surface after a 40-min bulk electrolysis in the presence of $[Co^{III}\mathbf{N_4H}(Br)_2]^+$ and CO_2 was determined via XPS on a Kratos Axis Nova spectrometer with DLD (Kratos Analytical; Manchester, UK). The excitation source for all analysis was monochromatic Al $K\alpha_{1,2}$ ($h\nu$ = 1486.6 eV) operating at 30 mA and 15 kV. The X-ray source was directed 45° with respect to the sample normal. A base pressure of 1×10^{-9} Torr is maintained in the analytical chamber, which rises to 5×10^{-9} Torr during spectral acquisition. All spectra were acquired using the hybrid lens magnification mode and slot aperture, resulting in an analyzed area of 700 μm × 400 μm. Survey scans were collected using 160 eV pass energy, while narrow region scans used 20 eV; charge compensation via the attached e^--flood source was not necessary in this study. The following sequence of scans was performed: Survey (−5–1200 eV), Na 1s (1068–1076 eV), O 1s (528–538 eV), Ag 3d (364–378 eV), C 1s (280–292 eV), Si 2s (146–161 eV) and Co 3p (52–70 eV).

Subsequent peak fitting and composition analysis was performed using CasaXPS version 2.3.16 (Casa Software Ltd.; Teignmouth, UK). Energy scale correction for the survey and narrow energy regions was accomplished by setting the large component in the C 1s spectrum, corresponding to a C 1s C(=C) transition, to 284.8 eV. All components were fitted using a Gaussian 30% Lorentzian convolution function. For quantification, Shirley baselines were employed where there was a noticeable change in CPS before and after the peak in the survey spectrum; otherwise, linear was chosen. Atomic percentages were calculated using the CasaXPS packages for regions and/or components and are reported herein. Calculations were performed using region or component areas normalized to relative sensitivity factors specific to the instrument conditions with deconvolution from the spectrometer transmission function.

Synthetic Methods. $[Co^{II}\mathbf{N_4H}(Br)]Br$ and $[Co^{III}\mathbf{N_4H}(Br)_2]Br$ were synthesized on a Schlenk line according to literature methods.[21] Remaining manipulations and syntheses were conducted in a Vacuum Atmospheres, Co. drybox under a nitrogen atmosphere. Solvents were dried using a JC-Meyer solvent system and otherwise degassed with N_2 before use. KC_8 and [H-DMF][OTf] were synthesized according to literature procedures.[38,39]

Preparation of $[Co^{II}\mathbf{N_4H}(Br)]Br$. Following a slightly modified procedure from Busch,[21] 2,6-diacetylpyridine (1.00 g, 6.13 mmol) and $CoBr_2$ (1.35 g, 6.17 mmol) were dissolved in 20 mL of degassed EtOH and treated with 0.5 mL of H_2O. Dropwise addition of 3,3′-diaminodipropylamine to the blue-

dx.doi.org/10.1021/ic403122j | Inorg. Chem. 2014, 53, 4980–4988

green solution caused the solution to become dark-red and opaque. After complete addition of 3,3′-diaminodipropylamine, the solution was treated with glacial acetic acid (1 μL), and the resulting dark-purple heterogeneous mixture was stirred for 12 h at 50 °C and afterward cooled to room temperature. The purple solid was collected on a glass fritted funnel and washed with Et_2O and dried over P_2O_5 for 24 h (2.5 g, 84%). FTIR-ATR: (solid powder, cm^{-1}) 3193, 3056, 2930, 2862, 1585, 1567. The elemental analysis match literature but are reported here for convenience: Anal. Calcd (found) for $[Co^{II}\mathbf{N_4H}(Br)]$-$Br{\cdot}0.5H_2O$ ($C_{15}H_{23}Br_2CoN_4O_{0.5}$): %C 37.06, (37.22); %H 4.77, (4.48); %N 11.53, (11.39). Post drying with P_2O_5 Anal. Calcd (found) for $[Co^{II}\mathbf{N_4H}(Br)]Br$ ($C_{15}H_{22}Br_2CoN_4$): %C 37.76, (37.28); %H 4.75, (4.93); %N 11.74, (11.35).

*Preparation of [Co^{III}**N$_4$H**(Br)$_2$]Br.* The salt $[Co^{III}\mathbf{N_4H}(Br)_2]Br$ was prepared according to literature procedures.[18] Aerobic oxidation of in situ prepared $[Co^{II}\mathbf{N_4H}(Br)_2]$ in the presence of 1 equiv $HBr_{(aq)}$ overnight afforded a green solution. Recrystallization was accomplished by diffusion of Et_2O into MeOH solutions of $[Co^{III}\mathbf{N_4H}(Br)_2]Br$. The solid was dried under reduced pressure with P_2O_5. ^{1}H NMR (MeOD-d_3, 400 MHz): δ 8.57 (3H, m, *Ar*-H), δ 6.43 (1H, t, *J* = 11.5, N*H*), δ 4.20 (2H, d, *J* = 16.4, C*H*), δ 3.65 (2H, t, *J* = 13.5, C*H*), δ 3.48 (2H, q, *J* = 11.5, C*H*), δ 3.12 (2H, d, *J* = 12.4, C*H*), δ 2.92 (6H, s, CH_3), δ 2.28 (4H, m, CH_2). Anal. Calcd (found) for $[Co^{III}\mathbf{N_4H}(Br)_2]Br$ ($C_{15}H_{22}Br_3CoN_4$): %C 32.34, (32.07); %H 3.98, (4.04); %N 10.06, (9.78).

*Preparation of [Co**N$_4$**].* Solid $[Co^{II}\mathbf{N_4H}(Br)]Br$ (294 mg, 0.616 mmol) and KC_8 (178 mg, 1.32 mmol) were placed in a 20 mL scintillation vial with a stir bar (the stir bar had been previously stirred over KC_8 in THF). THF (10 mL) was added at room temperature, and the vigorously stirring solution immediately became inky-purple and warm. Small amounts of bubbles were observed. After 30 min, the solution was filtered through Celite, and the filtrate was dried *in vacuo*. The solid was washed with 10 mL of toluene and passed through a medium porosity glass fritted funnel to remove insoluble material. The toluene was removed *in vacuo* to yield an analytically pure dark-purple solid (161 mg, 83%). X-ray quality crystals were grown by pentane vapor diffusion into a saturated benzene solution. The material could be further purified by saturating a solution in toluene and adding pentane and storing the solution at −35 °C for several days and washing the crystals with cold pentane on a glass fritted funnel (10% yield). To determine gaseous products, the reaction was conducted in a sealed flask, and THF solvent was added via syringe. By GC analysis, the amount of H_2 produced corresponded to a 20% yield based on $[Co\mathbf{N_4}]$ product. ^{1}H NMR (C_6H_6, 300 MHz): δ 8.15 (1H, t, *J* = 7.5 Hz, *Ar*-H), δ 7.62 (2H, d, *J* = 7.5 Hz, *Ar*-H), δ 4.28 (4H, br s, CH_2), δ 3.55 (4H, br s, CH_2), δ 2.25 (4H, br s, CH_2), δ 0.99 (6H, s, CH_3).^{13}C NMR (C_6H_6, 100 MHz) δ 117.3 (meta-C_{py}), δ 114.2 (para-C_{py}), δ 57.7 (CH_2), δ 53.4 (CH_2), δ 34.3 (CH_2), δ 17.0 (C_{Me}). FTIR-ATR: (cm^{-1}) 3105, 3070, 2905, 2808, 2745, 2663, 1571, 1530, 1510, 1485, 1446, 1380, 1355, 1337, 1317, 1260, 1194, 1177, 1152, 1136, 1125, 1013. UV−vis: λ_{max} (THF, nm (ε, $M^{-1}\,cm^{-1}$)) 375 (8300), 452 (shoulder, 2100), 544 (8300), 650 (1400), 773 (1750). Anal. Calcd (found) for $[Co\mathbf{N_4}]$ ($C_{15}H_{21}CoN_4$): %C 56.96 (56.69); %H 6.69 (6.79); %N 17.71 (17.51). Alternatively, solid $[Co^{II}\mathbf{N_4H}(MeCN)_2][BPh_4]_2$ (100 mg, 0.1 mmol) was suspended in 5 mL of THF and stirred with a stir bar that had been previously stirred over KC_8. The solution was treated with KC_8 (28 mg, 0.2 mmol) in two roughly equal portions causing the reaction to become dark inky-purple. After stirring for 5 min, 2 mL of pentane was added and allowed to stir for an additional 1 min after which the solution was passed through a filter pipet containing glass-fiber filter paper and a Celite pad, removing white/gray solid ($KBPh_4$ and C). The resulting homogeneous inky-purple filtrate was reduced to dryness in vacuo, and the resulting solid was treated with 5 mL benzene followed by 1 mL of pentane and again filtered through a filter pipet with glass wool. The resulting filtrate was reduced to dryness in vacuo (this process was repeated at least one more time). The resulting product was identical to $[Co\mathbf{N_4}]$ and analytically pure.

*Preparation of [Co**N$_4$H**(MeCN)][BPh$_4$].* Solid $[Co\mathbf{N_4}]$ (107 mg, 0.339 mmol) was dissolved in MeCN (15 mL) with $NaBPh_4$ (118 mg, 0.345 mmol), and degassed H_2O (2 mL) was added causing a color change from dark purple to dark green and was brought into an oxygen-free "wet" box. A small amount of water was added (∼0.5−5 mL) until crystallization was induced, and the resulting mixture was allowed to rest at room temperature for several days. The dark-green crystals were isolated on a glass fritted filter funnel and dried under reduced pressure for at least 12 h (149 mg, 65%). ^{1}H NMR (MeCN-d_3 400 MHz): δ 8.48 (1H, t, *J* = 7.7 Hz, *Ar*-H), δ 7.71 (2H, d, *J* = 7.7 Hz, *Ar*-H), δ 7.27 (8H, br s, *Ar*-H), δ 6.99 (8H, t, *J* = 7.3 Hz), *Ar*-H), δ 6.84 (4H, t, *J* = 7.1 Hz, *Ar*-H), δ 4.47 (2H, d, *J* = 14.2 Hz, C*H*), δ 3.29 (2H, t, *J* = 13.4 Hz, C*H*), δ 2.86 (2H, t, *J* = 11.3 Hz, C*H*), δ 2.75 (2H, q, *J* = 11.5 Hz, C*H*), δ 2.42 (1H, t, *J* = 11.5, N*H*), δ 2.22 (2H, d, *J* = 14.9, C*H*), δ 1.96 (s, coordinated MeCN), δ 1.82 (2H, q, *J* = 12.9, C*H*), δ 1.63 (6H, s, CH_3).^{13}C NMR (C_6H_6, 100 MHz) δ 164.8 (q, *J* = 49.5, B*Ph*$_4$), δ 148.2 (ortho-C_{py}) δ 136.7 (q, *J* = 1.34, B*Ph*$_4$), δ 126.6 (q, *J* = 2.65, B*Ph*$_4$), δ 124.6 (meta-C_{py}), δ 122.7 (B*Ph*$_4$), δ 116.6 (para-C_{py}), δ 54.2 (CH_2), δ 52.5 (CH_2), δ 29.6 (CH_2), δ 16.6 (C_{Me}). UV−vis: λ_{max} (MeCN, nm (ε, $M^{-1}\,cm^{-1}$)) 331 (6900), 430 (4750), 687 (1300), 845 (sh). FTIR-ATR: (cm^{-1}) 3251, 3047, 2979, 2935, 2920, 2873, 2840, 1579, 1475, 1426, 1386, 1306, 1257, 1142, 1060. Anal. Calcd (found) for $[Co\mathbf{N_4H}(MeCN)][BPh_4]$, $C_{41}H_{45}BCoN_5$: %C 72.68 (72.67); %H 6.69 (6.63); %N 10.34 (10.26).

*Yield of H$_2$ from Treatment of [Co**N$_4$H**(MeCN)][BPh$_4$] with [H-DMF][OTf].* Solid $[Co\mathbf{N_4H}(MeCN)][BPh_4]$ (20.0 mg, 0.030 mmol) was dissolved in 5 mL of MeCN in a 250 mL round-bottom flask and sealed. A stock solution of [H-DMF][OTf] in MeCN was added (1.0 mL, 30 mM), causing the immediate color change from dark green to orange-red. After 10 min, the headspace was sampled with a gas-tight syringe and injected into a GC. The yield was based on a calibrated method experiment (47% yield (±4%)).

*Preparation of [Co^{II}**N$_4$H**(MeCN)][OTf][BPh$_4$].* Solid $[Co^{II}\mathbf{N_4H}(MeCN)][BPh_4]$ (74.1 mg, 0.109 mmol) was dissolved in 5 mL of MeCN in a 20 mL vial. [H-DMF][OTf] (25.0 mg, 0.112 mmol) in 1 mL MeCN was added causing the immediate color change from dark green to orange-red. After 0.5 h the solution was layered under Et_2O affording red crystals (78.8 mg, 87%). μ_{eff} = 1.60 μ_B (MeCN-d_3, 20 °C). UV−vis: λ_{max} (MeCN, nm (ε, $M^{-1}\,cm^{-1}$)) 358 (990), 445 (1220), 450 (1210). FTIR-ATR: (cm^{-1}) 3235, 3082, 3048, 3026, 2995, 2982, 2940, 2924, 2886, 2873, 1582, 1478, 1464, 1426, 1366, 1326, 1286, 1251, 1237, 1220, 1170, 1157, 1144, 1093, 1077, 1064, 1051, 1024. Anal. Calcd (found) for $[Co^{II}\mathbf{N_4H}(MeCN)]$-[OTf][$[BPh_4]$, $C_{42}H_{45}BCoF_3N_5O_3S$: %C 61.02 (60.79); %H 5.49 (5.66) %N 8.47 (8.47).

*Preparation of [Co^{II}**N$_4$H**(MeCN)$_2$][BPh$_4$]$_2$.* Under a flow of N_2, solid $Co(BF_4)_2{\cdot}6H_2O$ (1.04 g, 3.1 mmol) and diacetyl-

dx.doi.org/10.1021/ic403122j | *Inorg. Chem.* 2014, 53, 4980−4988

pyridine (0.50 g, 3.1 mmol) were dissolved in 30 mL of degassed MeCN in a 500 mL Schlenk round-bottom flask. The pale-orange solution was treated dropwise with 3,3′-diaminodipropylamine (0.41 g, 3.1 mmol) in 5 mL of water (degassed) via addition funnel, and the solution turned slightly darker orange. The addition funnel was replaced under a stream of N_2 with a reflux condenser and heated to boiling upon which it turned from pale orange to very dark purple-red. The solution was refluxed overnight and afterward cooled to room temperature. The reflux condenser was replaced under a stream of N_2 with a new addition funnel and was treated dropwise with $NaBPh_4$ (2.00 g, 5.8 mmol) in 20 mL MeCN/H_2O (1:3) solution. The reaction mixture was exposed to vacuum and brought into a glovebox (wet-box) and treated with 40 mL of water, causing the precipitation of purple-red crystals which were isolated on a frit and washed one time with water and dried until a free-flowing powder. The solid was used to prepare a saturated MeCN solution (160 mL) of the compound and was recrystallized by slow diffusion of Et_2O, which yielded the pure compound as dark purple-black needles. The crystals were isolated on a glass fritted funnel and dried to constant weight at room temperature and analyzed as $[Co^{II}\mathbf{N_4H}(MeCN)_2][BPh_4]_2$ (yield 2.47 g = 78%). Anal. Calcd (found) for $[Co^{II}\mathbf{N_4H}(MeCN)_2][BPh_4]_2$, $C_{67}H_{68}B_2CoN_6$: %C 77.54 (77.05); %H 6.60 (6.55) %N 8.10 (8.06). When one equivalent (rather than excess) of $NaBPh_4$ was used in the synthesis, the product was obtained in 33% crystalline yield. Anal. Calcd (found) for $[Co^{II}\mathbf{N_4H}(MeCN)_2][BPh_4]_2$, $C_{67}H_{68}B_2CoN_6$: %C 77.54 (77.40); %H 6.60 (6.47) %N 8.10 (8.17). Spectroscopic measurements matched those obtained for $[Co^{II}\mathbf{N_4H}(MeCN)][OTf][BPh_4]$.

■ ASSOCIATED CONTENT

Supporting Information

Additional experimental details, UV−vis and FTIR and NMR spectra, computational details, and X-ray crystallographic information. This material is available free of charge via the Internet at http://pubs.acs.org.

■ AUTHOR INFORMATION

Corresponding Author

*E-mail: jpeters@caltech.edu

Notes

The authors declare no competing financial interest.

■ ACKNOWLEDGMENTS

This material is based upon work performed by the Joint Center for Artificial Photosynthesis, a DOE Energy Innovation Hub, supported through the Office of Science of the U.S. Department of Energy under Award Number DE-SC0004993. D.C.L. would also like to acknowledge the National Institutes of Health (Award Number F32GM106726). The authors would also like to thank Tzu-Pin Lin, Michael Takase, and Lawrence Henling for help with crystallography, and Kyle Cummins and Slobodan Mitrovic for help with XPS. Clifford Kubiak is also thanked for many insightful discussions.

■ REFERENCES

(1) Selected reviews on electrocatalytic CO_2 reduction (a) Scibioh, M. A.; Viswanathan, B. *Proc. Indian Natl.Sci. Acad.* **2004**, *70*, 1. (b) Schneider, J.; Jia, H.; Muckerman, J. T.; Fujita, E. *Chem. Soc. Rev.* **2012**, *41*, 2036. (c) Benson, E. E.; Kubiak, C. P.; Sathrum, A. J.; Smieja, J. M. *Chem. Soc. Rev.* **2009**, *38*, 89. (d) Costentin, C.; Robert, M.; Savéant, J.-M. *Chem. Soc. Rev.* **2013**, *42*, 2423.

(2) (a) Meshitsuka, S.; Ichikawa, M.; Tamaru, K. *J. Chem. Soc., Chem. Commun.* **1974**, 158. (b) Lieber, C. M.; Lewis, N. S. *J. Am. Chem. Soc.* **1984**, *106*, 5033.

(3) (a) Hiratsuka, K.; Takahashi, K.; Sasaki, H.; Toshima, S. *Chem. Lett.* **1977**, 1137. (b) Atoguchi, T.; Aramata, A.; Kazusaka, A.; Enyo, M. *J. Chem. Soc., Chem. Commun.* **1991**, 156. (c) Hammouche, M.; Lexa, D.; Momenteau, M.; Savéant, J.-M. *J. Am. Chem. Soc.* **1991**, *113*, 8455. (d) Costentin, C.; Drouet, S.; Robert, M.; Savéant, J.-M. *Science* **2012**, *338*, 90.

(4) (a) Hawecker, J.; Lehn, J.-M.; Ziessel, R. *J. Chem. Soc., Chem. Commun.* **1984**, 328. (b) Sullivan, P. B.; Bolinger, C. M.; Conrad, D.; Vining, W. J.; Meyer, T. J. *J. Chem. Soc., Chem. Commun.* **1985**, 1414. (c) Ishido, H.; Tanaka, H.; Tanaka, K.; Tanaka, T. *J. Chem. Soc., Chem. Commun.* **1987**, 131. (d) Bolinger, C. M.; Story, N.; Sullivan, B. P.; Meyer, T. J. *Inorg. Chem.* **1988**, *27*, 4582. (e) Rasmussen, S. C.; Richter, M. M.; Yi, E.; Place, H.; Brewer, K. J. *Inorg. Chem.* **1990**, *29*, 3926. (f) Ishida, H.; Fujiki, K.; Ohba, T.; Ohkubo, K. *J. Chem. Soc., Dalton Trans.* **1990**, 2155. (g) Chen, Z.; Chen, C.; Weinberg, D. R.; Kang, P.; Concepcion, J. J.; Harrison, D. P.; Brookhart, M. S.; Meyer, T. J. *Chem. Commun.* **2011**, *47*, 12607. (h) Chen, Z.; Kang, P.; Zhang, M.-T.; Meyer, T. J. *Chem. Commun.* **2014**, *50*, 335.

(5) (a) Fisher, B.; Eisenberg, R. *J. Am. Chem. Soc.* **1980**, *102*, 7363. (b) Schneider, J.; Jia, H.; Kobiro, K.; Cabelli, D. E.; Muckerman, J. T.; Fujita, E. *Energy Environ. Sci.* **2012**, *5*, 9502. (c) Thoi, V. S.; Kornienko, N.; Margarit, C. G.; Yang, P.; Chang, C. J. *J. Am. Chem. Soc.* **2013**, *135*, 14413.

(6) (a) Simpson, T. C.; Durand, R. R., Jr. *Electrochim. Acta* **1988**, *33*, 581. (b) Scheiring, T.; Klein, A.; Kaim, W. *J. Chem. Soc., Perkin Trans. 2* **1997**, 2569. (c) Fujita, E.; Muckerman, J. T. *Inorg. Chem.* **2004**, *43*, 7636. (d) Benson, E. E.; Sampson, M. D.; Grice, K. A.; Smieja, J. M.; Froehlich, J. D.; Friebel, D.; Keith, J. A.; Carter, E. A.; Nilsson, A.; Kubiak, C. P. *Angew. Chem., Int. Ed.* **2013**, *52*, 4841.

(7) Keith, J. A.; Grice, K. A.; Kubiak, C. P.; Carter, E. A. *J. Am. Chem. Soc.* **2013**, *135*, 15823.

(8) (a) Bourrez, M.; Molton, F.; Chardon-Nobalt, S.; Deronzier, A. *Angew.Chem., Int. Ed.* **2011**, *50*, 9903. (b) Smieja, J. M.; Sampson, M. D.; Grice, K. A.; Benson, E. E.; Roehlich, J. D.; Kubiak, C. P. *Inorg. Chem.* **2010**, *49*, 9283. (c) Smieja, J. M.; Kubiak, C. P. *Inorg. Chem.* **2013**, *52*, 2484.

(9) (a) Zhu, D.; Thapa, I.; Korobkov, I.; Gambarotta, S.; Budzelaar, P. H. M. *Inorg. Chem.* **2011**, *50*, 9879. (b) Knijnenburg, Q.; Gambarotta, S.; Budzelaar, P. H. M. *Dalton Trans.* **2006**, 5442. (c) Knijnenburg, Q.; Hetterscheid, D.; Kooistra, M.; Budzelaar, P. H. M. *Eur. J. Inorg. Chem.* **2004**, 1204. (d) Sieh, D.; Schlimm, M.; Andernach, L.; Angersbach, F.; Nückel, S.; Schöffel, J.; Susnjar, N.; Burger, P. *Eur. J. Inorg. Chem.* **2012**, 444. (e) Lu, C. C.; Weyhermuller, T.; Bill, E.; Wieghardt, K. *Inorg. Chem.* **2009**, *48*, 6055.

(10) (a) Ghosh, M.; Weyhermüller, T.; Wieghardt, K. *Dalton Trans.* **2010**, *39*, 1996. (b) Tait, A. M.; Lovecchio, F. V.; Busch, D. H. *Inorg. Chem.* **1977**, *16*, 2206.

(11) Arana, C.; Yan, S.; Keshavarz-K, M.; Potts, K. T.; Abruña, H. D. *Inorg.Chem.* **1992**, *31*, 3680.

(12) (a) Tinnemans, A. H. A.; Koster, T. P. M.; Thewissen, D. H. M. W.; Mackor, A. *Recl. Trav. Chim. Pays-Bas* **1984**, *103*, 288. (b) Che, C.-M.; Mak, S.-T.; Lee, W.-O.; Fung, K.-W.; Mak, T. C. W. *Dalton Trans.* **1988**, 2153.

(13) (a) Paul, N. *J. Electroanal. Chem.* **1967**, *14*, 197. (b) Baxter, L. A. M.; Bobrowski, A.; Bond, A. M.; Heath, G. A.; Paul, R. L.; Mrzljak, R.; Zarebski, J. *Anal. Chem.* **1998**, *70*, 1312. (c) Wenrui, J.; Kun, L. *J. Electroanal. Chem.* **1987**, *216*, 181.

(14) (a) Beley, M.; Collin, J. P.; Ruppert, R.; Sauvage, J. P. *J. Am. Chem. Soc.* **1986**, *108*, 7461. (b) Bujno, K.; Bilewicz, R.; Siegfried, L.; Kaden, T. A. *J. Electroanal. Chem.* **1998**, *445*, 47.

(15) Froehlich, J. D.; Kubiak, C. P. *Inorg.Chem.* **2012**, *51*, 3932.

(16) (a) Axolabéhere-Mallart, E.; Costentin, C.; Fournier, M.; Nowak, S.; Robert, M.; Savéant, J.-M. *J. Am. Chem. Soc.* **2012**, *134*, 6104. (b) Stracke, J. J.; Finke, R. G. *J. Am. Chem. Soc.* **2011**, *133*,

14872. (c) Soto, A. B.; Arce, E. M.; Palomar-Pardavé, M.; González, I. *Electrochim. Acta* **1996**, *41*, 2647.
(17) The remaining unaccounted charge could be ascribed to catalyst decomposition or nonproductive side reactions associated with the reduced cobalt complex. If one includes the two electrons needed to reduce the Co^{III} precatalyst to the Co^{I} state, then an overall Faradaic efficiency of 83% ± 9 is obtained.
(18) After a bulk electrolysis an aliquot of the solution was removed, and KOH was added to basify the solution. A 200 μL aliquot was diluted with 200 μL MeCN-d_3 and spiked with a DMF internal standard (the concentration of DMF was near the expected formate concentration based on current efficiency and charge passed during electrolysis), and the solution was probed with ^{1}H NMR spectroscopy. No formate resonance was detected. Alternatively, a 10 mL aliquot was removed after bulk electrolysis, and the solvent was removed *in vacuo*. The remaining solids were taken into 400 μL D_2O and a ^{13}C NMR spectrum was collected; no resonances consistent with oxalate, carbonate, or formate were detected.
(19) Cechal, J.; Luksch, J.; Konakova, K.; Urbanek, M.; Brandejsova, E.; Sikola, T. *Surf. Sci.* **2008**, *602*, 2693−2698.
(20) Marsh, D. A.; Yan, W.; Liu, Y.; Hemminger, J. C.; Penner, R. M.; Borovik, A. S. *Langmuir* **2013**, *29*, 14728−14732.
(21) (a) Long, M. K.; Busch, D. H. *Inorg.Chem.* **1970**, *9*, 505. (b) Tait, A. M.; Busch, D. H. *Inorg. Synth.* **1978**, *18*, 17−22.
(22) GC analysis of the headspace confirmed H_2 as an additional product (<20% yield based on [Co**N**$_4$] product). Reactions with 3 or more equiv of reductant gave intractable products.
(23) An NH resonance appears at 6.43 ppm (1H, t, $J_{N\text{-}H}$ = 11.5 Hz) for $[Co^{III}\mathbf{N_4H}(Br)_2]^+$ in methanol-d_3.
(24) Gibson, V. C.; Humphries, M. J.; Tellmann, K. P.; Wass, D. F.; White, A. J. P.; Williams, D. J. *Chem. Commun.* **2001**, 2252.
(25) (a) Bowman, A. C.; Milsmann, C.; Bill, E.; Lobkovsky, E.; Weyhermüller, T.; Wieghardt, K.; Chirik, P. J. *Inorg. Chem.* **2010**, *49*, 6110. (b) Yu, R. P.; Darmon, J. M.; Milsmann, C.; Margulieux, G. W.; Stieber, S. C. E.; Debeer, S.; Chirik, P. J. *J. Am. Chem. Soc.* **2013**, *135*, 13168.
(26) Fryzuk, M. D.; Leznoff, D. B.; Thompson, R. C.; Rettig, S. J. *J. Am. Chem. Soc.* **1998**, *120*, 10126.
(27) (a) Ingleson, M. J.; Pink, M.; Fan, H.; Caulton, K. G. *Inorg.Chem.* **2007**, *46*, 10321. (b) Fout, A. R.; Basuli, F.; Fan, H.; Tomaszewski, J.; Huffman, J. C.; Baik, M.-H.; Mindiola, D. J. *Angew. Chem., Int. Ed.* **2006**, *118*, 3369.
(28) Helm, M. L.; Stewart, M. P.; Bullock, R. M.; Dubois, M. R.; Dubois, D. L. *Science* **2011**, *333*, 863.
(29) The same amount of H_2 was obtained when excess acid was used. When 1/2 equiv acid was used, the yield of H_2 was reduced to 20% based on $[Co\mathbf{N_4H}(MeCN)]^+$.
(30) Varma, S.; Castillo, C. E.; Stoll, T.; Fortage, J.; Blackman, A. G.; Molton, F.; Deronzier, A.; Collomb, M.-N. *Phys. Chem. Chem. Phys.* **2013**, *15*, 17544.
(31) See Figure S10 of the SI for CV of isolated $[Co^{II}\mathbf{N_4H}(MeCN)]^{2+}$.
(32) Kosuke, I. *Acid-Base Dissociation Constants in Dipolar Aprotic Solvents*; Blackwell Scientific Publications: Oxford, 1990.
(33) Kaljurand, I.; Kütt, A.; Sooväli, L.; Rodima, T.; Mäemets, V.; Leito, I.; Koppel, I. A. *J. Org. Chem.* **2005**, *70*, 1019−1028.
(34) (a) Hu, X.; Cossairt, B. M.; Brunschwig, B. S.; Lewis, N. S.; Peters, J. C. *Chem. Commun.* **2005**, 4723. (b) Razavet, M.; Artero, V.; Fontecave, M. *Inorg. Chem.* **2005**, *44*, 4786. (c) Hu, X.; Brunschwig, B. S.; Peters, J. C. *J. Am. Chem. Soc.* **2007**, *129*, 8988. (d) Pantani, O.; Anxolabéhère-Mallart, E.; Aukauloo, A.; Millet, P. *Electrochem. Commun.* **2007**, *9*, 54. (e) Jacques, P.-A.; Artero, V.; Pecaut, J.; Fontecave, M. *Proc. Natl. Acad. Sci. U.S.A.* **2009**, *106*, 20627. (f) Dempsey, J. L.; Brunschwig, B. S.; Winkler, J. R.; Gray, H. B. *Acc. Chem. Res.* **2009**, *42*, 1995. (g) Fourmond, V.; Jacques, P.-A.; Fontecave, M.; Artero, V. *Inorg. Chem.* **2010**, *49*, 10338. (h) Berben, L. A.; Peters, J. C. *Chem. Commun.* **2010**, 398. (i) McCrory, C. C. L.; Uyeda, C.; Peters, J. C. *J. Am. Chem. Soc.* **2012**, *134*, 3164.
(35) (a) Adaev, I. S.; Korostoshevskaya, T. V.; Novikov, V. T.; Lysyak, T. V. *Russ. J. Electrochem.* **2005**, *41*, 1125. (b) Aga, H.; Aramata, A.; Hisaeda, Y. *J. Electroanal. Chem.* **1997**, *437*, 111.
(36) (a) Uyeda, C.; Peters, J. C. *J. Am. Chem. Soc.* **2013**, *135*, 12023. (b) Uyeda, C.; Peters, J. C. *Chem. Sci.* **2013**, *4*, 157.
(37) Leung, C.-F.; Chen, Y.-Z.; Yu, H.-Q.; Yiu, S.-M.; Ko, C.-C.; Lau, T.-C. *Int. J. Hydrogen Energy* **2011**, *36*, 11640.
(38) Berbreiter, D. E.; Killough, J. M. *J. Am. Chem. Soc.* **1978**, *100*, 2126.
(39) Favier, I.; Duñach, E. *Tetrahedron Lett.* **2004**, *45*, 3393.

dx.doi.org/10.1021/ic403122j | *Inorg. Chem.* 2014, 53, 4980−4988